ACS OMEGA

http://pubs.acs.org/journal/acsodf

Article

Spontaneous Condensation of RNA into Nanoring and Globular Structures

Jaime F. Ruiz-Robles, Adriana M. Longoria-Hernández, Nancy Gerling, Emmanuel Vazquez-Martinez, Luis E. Sanchez-Diaz, Ruben D. Cadena-Nava, Maria V. Villagrana-Escareño, Elizabeth Reynaga-Hernández, Boris I. Ivlev,* and Jaime Ruiz-Garcia*

Cite This: *ACS Omega* 2022, 7, 15404−15410

Read Online

ACCESS | Metrics & More | Article Recommendations

ABSTRACT: The effect of polyvalent cations, like spermine, on the condensation of DNA into very well-defined toroidal shapes has been well studied and understood. A great effort has been made to obtain similar condensed structures from RNA molecules, but so far, it has been elusive. In this work, we show that single-stranded RNA (ssRNA) molecules can easily be condensed into nanoring and globular structures on a mica surface, where each nanoring structure is formed mostly by a single RNA molecule. The condensation occurs in a concentration range of different cations, from monovalent to trivalent, but at a higher concentration, globular structures appear. RNA nanoring structures were observed on mica surfaces by atomic force microscopy (AFM). The samples were observed in tapping mode and were prepared by drop evaporation of a solution of RNA in the presence of one type of the different cations used. As far as we know, this is the first time that nanorings or any other well-defined condensed RNA structures have been reported in the presence of simple salts. The RNA nanoring formation can be understood by an energy competition between the hydrogen bonding forming hairpin stems—weakened by the salts—and the hairpin loops. This result may have an important biological relevance since it has been proposed that RNA is the oldest genome-coding molecule, and the formation of these structures could have given it stability against degradation in primeval times. Even more, the nanoring structures could have the potential to be used as biosensors and functionalized nanodevices.

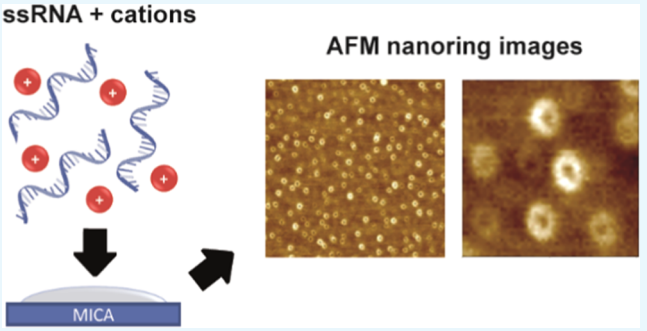

INTRODUCTION

Since Watson and Crick discovered the structure of the DNA,[1] its functions inside the cells, viruses, or bacteria have been investigated. The condensation of nucleic acids is an issue that has been fascinating scientists in diverse fields. Nucleic acid condensation is defined as the collapse of extended chains of DNA or RNA into highly ordered and compacted structures, which might have only one or a few molecules and that distinguishes it from random aggregation due to the high degree of order that molecules present within the condensed structure. Thus, the term condensation can be associated with the ordered aggregation of the nucleic acids into a limited size and well-defined morphology. Generally, the process of condensation of nucleic acids occurs mostly at the nanometric scale. The DNA condensation has been observed in cells,[2] spermatozoids,[3] bacteria,[4] and viruses.[5] But in recent decades, scientists' attention has gone to the study of RNA, which is the molecule directly involved in the protein's synthesis,[6] and it has a lot more functions inside the cell than DNA and it is also believed to be the precursor molecule of the origin of life.[7] The nucleic acid condensation is an issue that has direct importance in several research fields, such as cellular biology, virology, therapeutics, nanotechnology, and others.

In recent decades, studies have focused on trying to obtain condensed RNA structures to compare its behavior with DNA. One of the first observations on DNA condensation is its condensation in the cell's nucleus, where chromosomes are made up of DNA tightly wound around histone proteins, which order and pack the DNA into structural units known as nucleosomes.[8] DNA condensation into toroidal shapes has also been observed inside the bacteriophage capsids by the interaction with spermine.[9] In addition, it has been discovered that DNA condenses into rod-like and toroidal shapes in the presence of polyvalent cations in solution[10] or even inside liposomes.[11,12] Experimental evidence shows that DNA

Received: December 7, 2021
Accepted: April 7, 2022
Published: April 27, 2022

condensation occurs when 90% of its charge is neutralized by counterions.[10] There are several forces present in the DNA condensation phenomenon. The loss of entropy promotes the collapse; however, the major contributions are given by the multivalent molecular cations in the solution. DNA condensates form well-defined structures regardless of DNA size, and these structures are preferably in the shape of toroids of similar sizes.

Thus, the addition of small amounts of multivalent molecular cations to solutions containing double-stranded DNA leads to inter-DNA attraction and its eventual condensation. Surprisingly, an expected similar condensation is suppressed in double-stranded RNA (dsRNA), which carries a similar negative charge density as DNA but assumes a different double-helical form.[13] Thus, highly charged DNA molecules are expected to repel each other, and yet can be condensed by certain multivalent cations into structured aggregates.[10−12] The condensation phenomenon is biologically important since the compaction of anionic DNA and RNA molecules by oppositely charged cationic agents enables efficient packaging of the genetic material inside living cells and viruses. It has been shown that the intramolecular attraction of DNA is mainly due to electrostatic contributions in the presence of multivalent cations. However, dsRNA helices resist condensation under conditions where DNA duplexes condense easily.[14] The condensation of single-stranded RNA (ssRNA) by multivalent molecular cations has also been attempted; however, so far, there is no evidence of well-defined structural condensation of ssRNA.[15] The reason might be that ssRNA in solution presents secondary or tertiary structures, which fluctuate. Although there is a minimum free energy (MFE) secondary structure, as shown in Figure 1, there

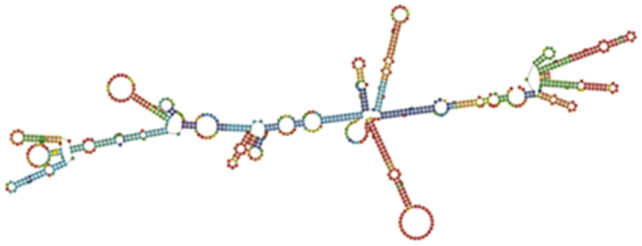

Figure 1. Minimum free energy secondary structure of the RNA that codes for an enhanced green fluorescent protein (EGFP) obtained by the Vienna RNA software package.

are other structures that are very close in energy to the MFE secondary structure. Therefore, the structure of the ssRNA fluctuates between different structures, and obtaining a well-defined compact condensed structure is not expected.

In this work, we prepare ssRNA solutions with monovalent, divalent, and trivalent atomic cations, from 1 to 15 mM salt concentrations. The salts used acted as chaotropic agents, helping in the disruption of the ssRNA secondary structure because the salts weaken the hydrogen bonds. After depositing the RNA solution on the mica surface, the samples were observed by atomic force microscopy (AFM), which revealed the formation of RNA nanorings. The nanorings are mostly one molecule thick, but the estimated number of RNA molecules forming the nanorings depends on the valence of the cation. Furthermore, when the cation concentration increases, globular RNA structures are formed. As far as we know, this is the first report on the formation of well-defined condensed structures of RNA molecules.

MATERIALS AND METHODS

Five different mRNA molecules were used in this study; four of them were purified from the CCMV virus, which contains an RNA mixture composed of RNA1 (3171 nucleotides (nt)), RNA2 (2774 nt), RNA3 (2173 nt), and RNA4 (824 nt),[16] and the entire RNA mixture was used directly. The fifth RNA molecule used was a pure RNA encoding the enhanced green fluorescent protein (EGFP) with a sequence length of 798 nucleotides, where its MFE secondary structure is shown in Figure 1. The EGFP was cloned into the Eco RI site of pVAX1, as has been described before.[17] Briefly, the plasmid pVAX1-EGFP was amplified and purified using a Qiagen Maxi kit (QIAGEN, Valencia CA). RNA transcription in vitro was carried out by a RiboMAX large-scale RNA production system kit (Promega, Madison WI). A total of 40 μg of pVAX1-EGFP was linearized with Xho I (NEB, Ipswich, MA) at 37 °C and inactivated at 65 °C, then the linearized plasmid was extracted with phenol:chloroform, precipitated with alcohols, and eluted in nuclease-free water. Overall, 10 μg of this DNA was subjected to a T7 transcription reaction in 20 μL, as indicated by the manufacturer. The RNA transcript was treated with RQ1 RNase-free DNase (1 U/μg) for 15 min at 37 °C followed by a phenol:chloroform purification protocol and eluted in nuclease-free water. In the purification protocol, the RNA was precipitated with isopropanol plus 3 M sodium acetate or 90% ethanol followed by a 70% ethanol rinse. The integrity of mRNA was evaluated by denatured gel electrophoresis with formaldehyde in 1× MOPS as a running buffer with diethylpyrocarbonate (DEPC) water. The in vitro transcripts were denatured for 15 min at 65 °C and then kept on ice for 5 min before they were loaded onto a 1.2% agarose gel. The mRNA was compared with a ssRNA ladder (NEB, Ipswich, MA). To prevent RNA degradation, the RNA molecules were kept in a buffer that consists of 0.9 M NaCl, 0.02 M Tris−HCl, and 0.01 M EDTA at pH 7.0. For all RNA samples, purity and concentration were determined by UV−vis spectrophotometer measurements (NanoDrop 2000C, Thermo-Scientific, MA). A curve of the sample absorbance was obtained and compared with the characteristic values of RNA. The purity of the RNA sample is calculated as $P = A_{260}/A_{280}$, where A_{260} and A_{280} are the absorbances at 260 and 280 nm, respectively, and P is the RNA purity value.[18] For RNA, the purity is considered good enough when this ratio is at least 1.5 with a maximum at 260 nm.[18] The virus concentration is obtained by $C = A_{260} \times 40$ μg/mL. For the RNA samples used in this work, the absorbance at 260 nm was 1.75, which means that the concentration of the sample was 70.13 μg/mL and the purity was 2.13. After verifying that the RNA purity was very good, the RNA was stored in a sterilized 1.5 mL RNase-free tube and placed in the freezer at −80 °C to prevent RNA degradation.

All of the materials used for the sample preparation were RNase-free and properly sterilized. Buffer solutions were prepared with monovalent (NaCl), divalent ($MgCl_2$), or trivalent ($CeCl_3.7H_2O$) salts at 5, 10, 12, and 15 mM concentrations for each salt using autoclaved deionized water (>18 MΩ/cm). RNA dilutions were prepared at concentrations of 0.07 mg/mL in nuclease-free water (NFW). A total of 5 μL of the RNA solution was aggregated into a 1.5 mL RNase-free tube with 1 mL of every correspondent salt

https://doi.org/10.1021/acsomega.1c06926
ACS Omega 2022, 7, 15404−15410

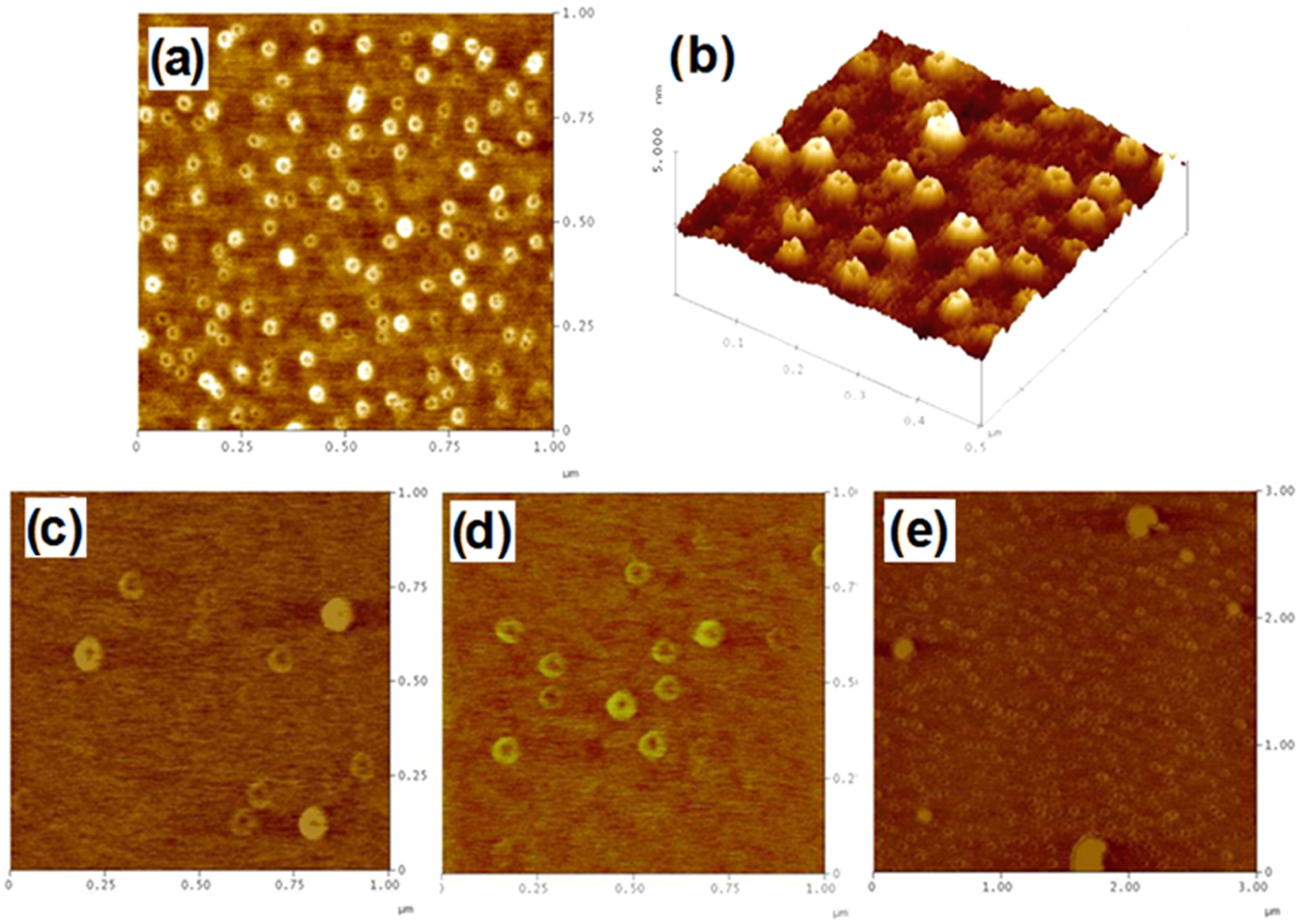

Figure 2. CCMV RNA nanoring structures. (a) Atomic force microscopy (AFM) image of the four CCMV RNA mixture at a high concentration forming nanorings observed at 12 mM NaCl. (b) Three-dimensional (3D) image of a section of the nanoring image of (a) showing details on the difference in the height of the nanorings. AFM images of the four CCMV RNA mixture forming nanorings observed at (c) 12 mM Na^{+}, (d) 12 mM Mg^{2+}, and (e) 5 mM Cs^{3+}.

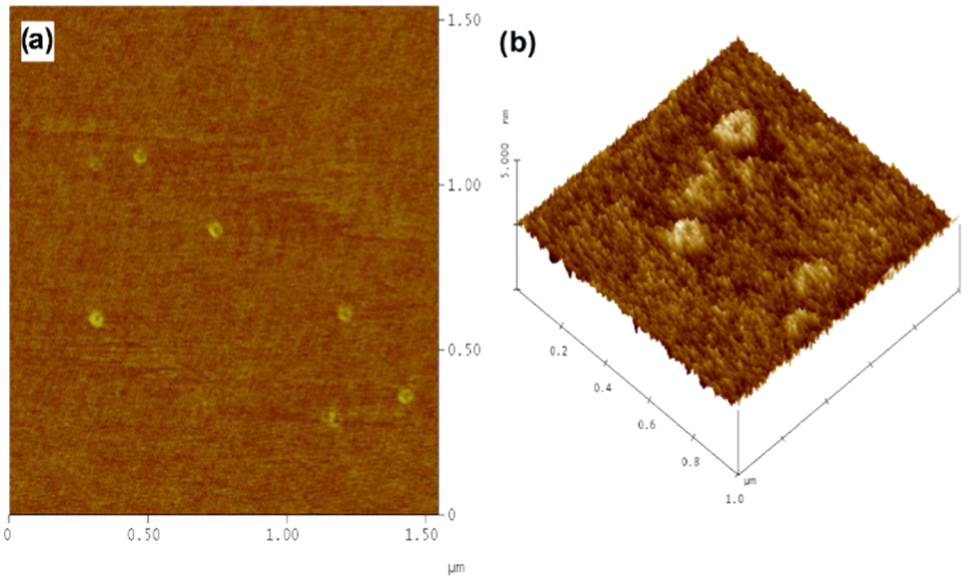

Figure 3. AFM nanoring images formed by EGFP RNA observed in the presence of different cations or concentrations. (a) 15 mM Mg^{2+} and (b) 5 mM Na^{+}.

solution and mixed gently for RNA dissolution. The final RNA solutions with the three different salts used were deposited onto freshly cleaved mica and dried at ambient temperature without disturbance.

https://doi.org/10.1021/acsomega.1c06926
ACS Omega 2022, 7, 15404−15410

Table 1. Size Characteristics of the Nanoring Formed by the CCMV RNAs Observed by AFM at Different Molar Concentrations of the Salts Used

ion salt	Na^+				Mg^{2+}				Cs^{3+}	
concentration (mM)	5	10	12	15	5	10	12	15	1	5
external diameter (D_{ext} (nm))	56 ± 4.1	47 ± 3.8	43 ± 3.5	58 ± 4.0	48 ± 3.3	82 ± 4.5	74 ± 4.5	72 ± 4.3	63 ± 3.8	77 ± 4.5
molecules/nanoring	1.6 ± 0.2	1.2 ± 0.2	0.9 ± 0.2	1.7 ± 0.3	1.2 ± 0.1	3.4 ± 0.2	2.8 ± 0.2	2.7 ± 0.3	2.1 ± 0.2	3.0 ± 0.3
nanoring height (nm)	2.6 ± 0.3	1.5 ± 0.3	1.1 ± 0.2	1.2 ± 0.2	1.2 ± 0.1	2.3 ± 0.2	1.5 ± 0.1	2.2 ± 0.2	4.3 ± 0.3	4.4 ± 0.3

Samples were imaged using a Nanoscope III Multimode AFM equipped with a piezoelectric scanner, with a maximum scan range of 10 μm (x and y) and 3.8 μm (z) (VEECO/Digital Instruments). Images were obtained in a tapping mode (oscillation frequency 250−300 kHz) under ambient conditions, using microcantilevers (MikroMash, Watsonville, CA) with a nominal radius of curvature <10 nm, a spring constant of 48 N/m, and a resonance frequency of 325 kHz. The scan rates used were 1−3 Hz and the images were acquired at 512 × 512 pixels. The samples were usually imaged immediately after drying the sample, but some samples were imaged within a few days after preparation. Samples were stored at 4 °C, and images of some samples were taken 1 month after preparation to study any changes in morphology.

RESULTS AND DISCUSSION

RNA samples were deposited on freshly cleaved mica, which is a widely used substrate for the deposition of biomolecules to be observed by AFM due to its molecularly flat and smooth surface. The typical roughness observed on the mica surface is about 0.09 nm.[19] However, when the surface of the freshly cleaved mica comes in contact with a water solution, the hydrated potassium ions desorb, causing the surface of the mica to acquire a negative charge.[20] Since RNA in a buffer solution also acquires a highly negative charge, it is important to have positive ions in the RNA buffer solution. Therefore, the positive ions in the solution have two important effects in our experiments; the first one is that they act as chaotropic agents, as discussed below. The second effect is to neutralize or even reverse the mica surface charge to a positive surface that facilitates the absorption of the RNA molecules; thus, the cations from the salt not only neutralize the mica surface charge but in the case of multivalent cations can reverse the mica surface charge and facilitate the adhesion of the nucleic acid. In addition, we use a low concentration of salts to prevent the formation of salt crystals on the mica surface.[21]

Nanoring structures were observed after a few μL of the RNA solution with cationic ions is deposited on a recently cleaved mica surface, as shown in Figures 2 and 3, where Figure 2 was obtained at a higher concentration of RNA than Figure 3. The nanoring structures are quite well defined, although in Figure 2 some nanorings seem to be smaller and less thick. This could be due to the CCMV mixture of RNA3 and RNA4 being much smaller than RNA1 and RNA2. In addition, it can be observed that between the nanoring structures, there is RNA material that is not fully incorporated into the nanoring structures. Figure 2c−e also shows the formation of nanorings from the CCMV RNA mixture, with the three different cations used. It is important to mention that most nanoring structures are made mostly by one up to three RNA molecules. The separation of the nanoring structures could be explained by a wetting effect that can break down due to capillary instabilities, where the adsorbed film decomposes into a collection of segregated, nonoverlapping molecules.[22] Figure 3 shows nanoring structures obtained with EGFP RNA with (a) Mg^{2+} and (b) Na^+. It is worth mentioning that similar, but much bigger, nanoring structures have been observed when a mixture of a cationic polymer, e.g. polyethylenimine (PEI), is mixed with an anionic polymer, poly(sodium 4-styrenesulfanate) (PSS), and also when a third polyelectrolyte is added into the previous polyelectrolyte mixture such as polyallylamine hydrochloride (PAH).[23,24]

Table 1 shows the sizes of the CCMV RNA nanoring structures under different conditions in which the experiments were performed. Note that the external diameter of the nanorings (D_{ext}) for the monovalent cationic salt is very similar at all concentrations used, which is also of similar size for the divalent cationic salt at the two lower concentrations. Using the thickness of the nanoring and the external and internal diameter, we estimated that these nanorings are approximately made by one RNA molecule. However, when the concentration of the divalent cationic salt increases, the size of the nanorings also increases. However, the size of the nanorings is greater, as is the number of molecules involved in the formation of the nanorings, with the trivalent salt even at low concentrations.

In general, the thickness of the nanorings for the monovalent and divalent cationic salts, at a low concentration, corresponds to the thickness of one RNA molecule (~1 nm). However, the thickness increases as the salt concentration increases, especially with the divalent and trivalent cationic salts. Even more, at higher concentrations of divalent or trivalent salts, the nanorings fill up, increase in size, and begin to have a more spherical shape, but are still well separated from each other, as shown in Figure 4. This observation is consistent with the formation of a compacted RNA tertiary structure.

It should be noted that toroidal DNA condensation is only observed in the presence of multivalent molecular cations in solution, whereas, here, we report RNA condensation in the presence of monovalent to trivalent atomic cations. This condensation can be understood as a competition of the energy related to the two types of hairpins that form the RNA secondary structure, as shown schematically in Figure 5.

The left part in Figure 5 is formed when two strands are bounded by hydrogen bonds, two or three depending on the nucleotide pairing, where the nucleotides are separated by the distance "a" and this arrangement is commonly called a hairpin stem. The energy related to the hairpin stem can be described by the following expression

$$E_{hyd} = -V_{hyd}\frac{L - n^2\pi R}{2a} \quad (1)$$

where L is the total length of RNA, V_{hyd} is the energy gain due to the formation of individual hydrogen bonds, and n is the average number of nucleotides in the hairpin loops formed in the RNA secondary structure. In the hairpin loop part, the

https://doi.org/10.1021/acsomega.1c06926
ACS Omega 2022, 7, 15404−15410

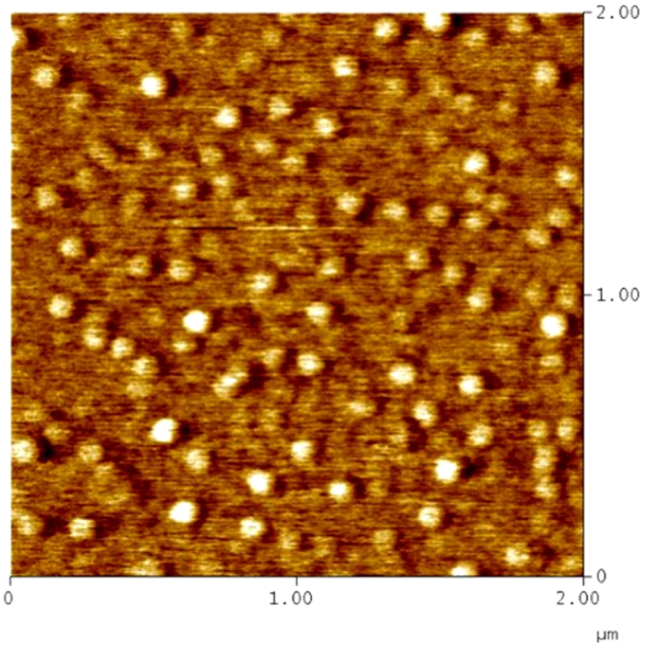

Figure 4. AFM image of RNA globules observed at 20 mM Mg^{2+}. The average diameter of these structures is 102.7 ± 5.5 nm and their average height is 1.4 ± 0.15 nm.

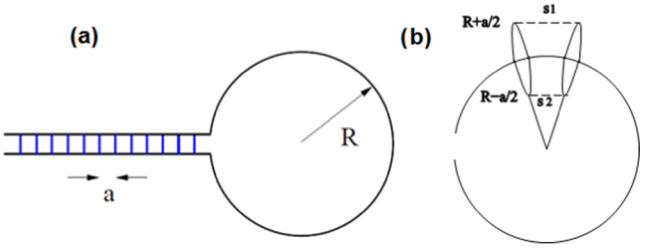

Figure 5. Schematic representation of the main structures of the ssRNA secondary structure. (a) Schematic organization of a hairpin stem and a hairpin loop. The hairpin stem on the left part contains hydrogen bonds and the nucleotides are separated by the distance $a \sim 1$ nm due to base pairing when read in opposite directions. Whereas, R is the radius of the hairpin loop. (b) Schematic figure of the part of the bent chain of nucleotides in the hairpin loop, where the distance between two nucleotides along the hairpin loop is "a".

hydrogen bonds are not involved. Instead, there is an elastic energy pay due to the bending of the RNA chain. This elastic energy can be evaluated from general arguments. In the hairpin loop, as shown in Figure 5b, the average center-to-center distance between nucleotides can be estimated as

$$S_{1,2} = a \pm \frac{a^2}{2R} \tag{2}$$

When R becomes very large (no bending), the position is equilibrium related to the minimum of the covalent energy. The deviation from this equilibrium value (elastic energy E_{el}) is quadratic with respect to the displacement $a^2/2R$. Then, the elastic energy can be written in the following form

$$E_{el} = \alpha \frac{V_{cov}}{a^2}\left(\frac{a^2}{2R}\right)^2 \frac{2\pi R}{a} \tag{3}$$

where α is a numerical parameter and the last factor represents the total number of sites along the circle. V_{cov} is the individual covalent energy of one site. As a result, the elastic energy of the circle can be written as

$$E_{el} = \frac{\pi\alpha}{2} V_{cov} \frac{a}{R} \tag{4}$$

The total energy, $E_{hyd} + E_{el}$, can be minimized with respect to R to obtain the equilibrium circle radius. The result is

$$R = a\sqrt{\frac{\alpha}{2}\frac{V_{cov}}{V_{hyd}}} \tag{5}$$

V_{hyd} becomes even weaker in the presence of the chaotropic salts, so the radius of the RNA circle (Nanoring) is much greater than the distance $a \leq 1$ nm between the subsequent RNA nucleotides. Since the energy of the C−C bond is of the order of 347 KJ/mol[25] and the hydrogen bonds are of the order of 10−40 KJ/mol,[26] then, in this case, we can take the lower value due to the presence of the chaotropic salts to estimate the value of the constant α. Taking an average diameter value of the nanorings of ∼60 nm, the value for the constant α is of the order of 207.

An interesting question is how the ionic concentration influences the shape of the hairpins. In the model presented, the constant α in eq 3 remains as a fitting parameter. This constant is determined by the interaction strength of the nucleotides in Figure 1. This interaction definitely depends on the ionic concentration. The screening effect of the ions reduces the effective interaction by decreasing this constant, which results in a reduction of the radius R in Figure 5. This mechanism correlates well with the effects that ions have on flexible polyelectrolytes in solution, where a high ionic concentration leads to a highly compact shape of a bent chain system.[27,28] At room temperature, k_BT is of the order of 5−10% of the energy of the hydrogen bonds, which are of the order of 0.1−0.4 eV. Thus, the entropic effects are just a correction to the main result determined by the energy minimization.

CONCLUSIONS

In this work, we resolved the question of whether or not ssRNA molecules could be condensed into well-defined structures; this is, the condensation of RNA molecules by multivalent molecular cations into well-defined structures, similar to those obtained for DNA by similar cations. Attempts have been made to obtain these well-defined condensed structures on both types of molecules, ssRNA and dsRNA, without success. It has also been recognized that the DNA's internal structure plays an important role in its well-defined toroidal condensation.[29] Even though dsRNA has a similar number of charges as dsDNA, no well-defined structures have been observed so far. On the other hand, ssRNA has many secondary structures because these structures only differ very little from the secondary structure of the minimum global energy. Therefore, the RNA structure fluctuates among different secondary structures, and these differences might prevent the formation of well-defined structures.

RNA plays a very important role in various cellular activities and many of its biological functions depend on its three-dimensional structure, for example, RNA condensation within viral capsids is very important. We study different RNA molecules, with different lengths and secondary structures. We show for the first time, the formation of condensed structures in ssRNA in the form of nanorings and globular structures on

https://doi.org/10.1021/acsomega.1c06926
ACS Omega 2022, 7, 15404−15410

planar substrates. The formation of these RNA nanostructures can be understood by the energy minimization of the RNA molecules; this is, the competition between the elastic energy due to the bending of the RNA chain in the hairpin loop and the hydrogen bonding in the hairpin stem, where the hydrogen bond energy is weakened by the interaction with the chaotropic salts, breaking or disrupting the hydrogen bonds of the RNA secondary structure. Furthermore, they could prevent the dissociation of ions along the RNA chain, increasing the hydrophobicity regions along the RNA chain. The RNA molecules will then try to hide their hydrophobic groups by forming the nanoring structure, starting the structure with the shape of the hairpin loops. Also, the concentration of salts is important, since without or at relatively high concentrations of salts, the formation of RNA nanorings is not observed. On the other hand, if the salt concentration is high, the formation of RNA globules is observed instead of nanorings. Our work is the first one to present well-defined condensed structures of ssRNA. These advances could facilitate the structural understanding of many aspects of RNA biology, since the observation of the formation of the RNA nanoring and globular structures could lead to a better understanding of the stability of RNA molecules, especially in primeval times, since it has been proposed that RNA was the first genetic molecule that gave rise to life.[6] Even more, nanobiotechnology has continued to improve and the RNA nanoring or globule nanoparticle structures could be used as biosensors and functionalized nanodevices.[30]

AUTHOR INFORMATION

Corresponding Authors

Boris I. Ivlev − *Biological Physics Laboratory, Institute of Physics, Universidad Autónoma de San Luis Potosí, San Luis Potosí 78000, San Luis Potosí, México*; Email: ivlev@mail.ifisica.uaslp.mx

Jaime Ruiz-Garcia − *Biological Physics Laboratory, Institute of Physics, Universidad Autónoma de San Luis Potosí, San Luis Potosí 78000, San Luis Potosí, México*; orcid.org/0000-0003-3730-3825; Email: jaime@mail.ifisica.uaslp.mx

Authors

Jaime F. Ruiz-Robles − *Biological Physics Laboratory, Institute of Physics, Universidad Autónoma de San Luis Potosí, San Luis Potosí 78000, San Luis Potosí, México;* Present Address: J.F.R.-R.: Archaeomaterials Group & Molecular and Nano Archaeology Laboratory, UCLA Henry Samueli School of Engineering and Applied Science, 7400 Boelter Hall Los Angeles, CA 90095, USA

Adriana M. Longoria-Hernández − *Biological Physics Laboratory, Institute of Physics, Universidad Autónoma de San Luis Potosí, San Luis Potosí 78000, San Luis Potosí, México;* Present Address: A.M.L.-H.: Institute of Renewable Energies-UNAM, Priv. Xochicalco S/N Temixco, Morelos 62580, México.

Nancy Gerling − *Biological Physics Laboratory, Institute of Physics, Universidad Autónoma de San Luis Potosí, San Luis Potosí 78000, San Luis Potosí, México*

Emmanuel Vazquez-Martinez − *Biological Physics Laboratory, Institute of Physics, Universidad Autónoma de San Luis Potosí, San Luis Potosí 78000, San Luis Potosí, México*

Luis E. Sanchez-Diaz − *Biological Physics Laboratory, Institute of Physics, Universidad Autónoma de San Luis Potosí, San Luis Potosí 78000, San Luis Potosí, México;* Present Address: L.E.S.-D.: Chemistry and Physics Department, University of Tennessee at Chattanooga, 615 McCallie Ave, Chattanooga, TN 37403, USA.

Ruben D. Cadena-Nava − *Biological Physics Laboratory, Institute of Physics, Universidad Autónoma de San Luis Potosí, San Luis Potosí 78000, San Luis Potosí, México;* Present Address: R.D.C.-N.: Center of Nanosciences and Nanotechnology-UNAM, Km 107 Carretera Tijuana-Ensenada, Ensenada, B.C. 22800, México.

Maria V. Villagrana-Escareño − *Biological Physics Laboratory, Institute of Physics, Universidad Autónoma de San Luis Potosí, San Luis Potosí 78000, San Luis Potosí, México*

Elizabeth Reynaga-Hernández − *Biological Physics Laboratory, Institute of Physics, Universidad Autónoma de San Luis Potosí, San Luis Potosí 78000, San Luis Potosí, México*

Complete contact information is available at: https://pubs.acs.org/10.1021/acsomega.1c06926

Author Contributions

J.F.R.-R., A.M.L.-He., N.G., E.V.-M., and L.E.S.-D. performed the experiments on the formation of the RNA nanoring structures on mica and their observation by AFM; R.D.C.-N., M.V.V.-E., and E.R.-H. purified the RNA from the CCMV virus and performed the experiments to obtain the EGFP RNA; B.I.I. developed the theory to explain the RNA nanoring formation and funding acquisition; and J.R.-G. directed the project and experiments and contributed to funding acquisition. All authors contributed to the revision of the manuscript. This manuscript was written through contributions of all authors. All authors have given approval to the final version of the manuscript.

Notes

The authors declare no competing financial interest.

ACKNOWLEDGMENTS

The authors acknowledge support from the Consejo Nacional de Ciencia y Tecnología (CONACYT-Mexico) through grants FC-341, CB-254981, and CB-237439. J.R.-G. also acknowledges partial support from the UASLP through the Fondos Concurrentes program.

REFERENCES

(1) Watson, J. D.; Crick, F. H. Molecular Structure of Nucleic Acids: A Structure for Deoxyribose Nucleic Acid. *Nature* **1953**, *171*, 737−738.

(2) Luger, K.; Mäder, A. W.; Richmond, R. K.; Sargent, D. F.; Richmond, T. J. Crystal structure of the nucleosome core particle at 2.8 Å resolution. *Nature* **1997**, *389*, 251−260.

(3) Miller, D.; Brinkworth, M.; Iles, D. Paternal DNA packaging in spermatozoa: more than the sum of its parts? DNA, histones, protamines and epigenetics. *Reproduction* **2010**, *139*, 287−301.

(4) de Vries, R. DNA condensation in bacteria: Interplay between macromolecular crowding and nucleoid proteins. *Biochimie* **2010**, *92*, 1715−1721.

(5) Leforestier, A.; Livolant, F. Structure of toroidal DNA collapsed inside the phage capsid. *Proc. Natl. Acad. Sci.* **2009**, *106*, 9157−9162.

(6) Lodish, H.; Berk, A.; Zipursky, S. L.; Matsudaira, P.; Baltimore, D.; Darnell, J. The Three Roles of RNA in Protein Synthesis. In *Molecular Cell Biology*, 4th ed.; W. H. Freeman and Company, 2000.

(7) Gilbert, W. Origin of life: The RNA world. *Nature* **1986**, *319*, 618.

https://doi.org/10.1021/acsomega.1c06926
ACS Omega 2022, 7, 15404−15410

(8) Annunziato, A. DNA packaging: nucleosomes and chromatin *Nat. Educ.* 2008, *1*, 26 31.
(9) Leforestier, A.; Šiber, A.; Livolant, F.; Podgornik, R. Protein-DNA interactions determine the shapes of DNA toroids condensed in virus capsids. *Biophys. J.* **2011**, *100*, 2209−2216.
(10) Bloomfield, V. A. DNA condensation by multivalent cations. *Biopolymers* **1997**, *44*, 269−282.
(11) Gelbart, W. M.; Bruinsma, R. F.; Pincus, P. A.; Parsegian, V. A. DNA-inspired electrostatics. *Phys. Today* **2000**, *53*, 38−45.
(12) Lambert, O.; Letellier, L.; Gelbart, W. M.; Rigaud, J. L. DNA delivery by phage as a strategy for encapsulating toroidal condensates of arbitrary size into liposomes. *Proc. Natl. Acad. Sci.* **2000**, *97*, 7248−7253.
(13) Tolokh, I. S.; Pabit, S. A.; Katz, A. M.; Chen, Y.; Drozdetski, A.; Baker, N.; Pollack, L.; Onufriev, A. V. Why double-stranded RNA resists condensation. *Nucleic Acids Res.* **2014**, *42*, 10823−10831.
(14) Li, L.; Pabit, S. A.; Meisburger, S. P.; Pollack, L. Double-stranded RNA resists condensation. *Phys. Rev. Lett.* **2011**, *106*, No. 108101.
(15) Scheel, B.; Teufel, R.; Probst, J.; Carralot, J. P.; Geginat, J.; Radsak, M.; Jarrossay, D.; Wagner, H.; Jung, G.; Rammensee, H-G.; Hoerr, I.; Pascolo, S. Toll-like receptor-dependent activation of several human blood cell types by protamine-condensed mRNA. *Eur. J. Immunol.* **2005**, *35*, 1557−1566.
(16) Allison, R. F.; Janda, M.; Ahlquist, P. Infectious in vitro transcripts from cowpea chlorotic mottle virus cDNA clones and exchange of individual RNA components with brome mosaic virus. *J. Virol.* **1988**, *62*, 3581−3588.
(17) Villagrana-Escareño, M. V.; Reynaga-Hernández, E.; Galicia-Cruz, O. G.; Durán-Meza, A. L.; de la Cruz-González, V.; Hernández-Carballo, C. Y.; Ruiz-Garcia, J. VLPs derived from the CCMV plant virus can directly transfect and deliver heterologous genes for translation into mammalian cells. *BioMed Res. Int.* **2019**, *2019*, No. 4630891.
(18) Michel, J. P.; Gingery, M.; Lavelle, L. Efficient purification of bromoviruses by ultrafiltration. *J. Virol. Methods* **2004**, *122*, 195−198.
(19) Sasou, M.; Sugiyama, S.; Yoshino, T.; Ohtani, T. Molecular flat mica surface silanized with methyltrimethoxysilane for fixing and straightening DNA. *Langmuir* **2003**, *19*, 9845−9849.
(20) Leng, Y.; Cummings, P. T. Hydration structure of water confined between mica surfaces. *J. Chem. Phys.* **2006**, *124*, No. 074711.
(21) Bustamante, C.; Rivetti, C. Visualizing protein-nucleic acid interactions on a large scale with the scanning force microscope. *Annu. Rev. Biophys. Biomol. Struct.* **1996**, *25*, 395−429.
(22) Nguyen, T. T.; Bruinsma, R. F. RNA condensation and the wetting transition. *Phys. Rev. Lett.* **2006**, *97*, No. 108102.
(23) Menchaca, J. L.; Flores, H.; Cuisinier, F.; Pérez, E. Self-assembled polyelectrolyte nanorings observed by liquid-cell AFM. *J. Phys.: Condens. Matter* **2004**, *16*, S2109−S2117.
(24) Flores, H.; Menchaca, J. L.; Tristan, F.; Gergely, C.; Pérez, E.; Cuisinier, F. J. Polyelectrolyte nanoring structures: critical parameters governing formation and structural analysis. *Macromolecules* **2005**, *38*, 521−526.
(25) Blanksby, S. J.; Ellison, G. B. Bond dissociation energies of organic molecules. *Acc. Chem. Res.* **2003**, *36*, 255−263.
(26) Vušurović, J.; Breuker, K. Relative Strength of Noncovalent Interactions and Covalent Backbone Bonds in Gaseous RNA−Peptide Complexes. *Anal. Chem.* **2019**, *91*, 1659−1664.
(27) Solis, F. J.; Olvera de la Cruz, M. Collapse of flexible polyelectrolytes in multivalent salt solutions. *J. Chem. Phys.* **2000**, *112*, 2030−2035.
(28) Sun, L. Z.; Zhou, Y.; Chen, S. J. Predicting monovalent ion correlation effects in nucleic acids. *ACS Omega* **2019**, *4*, 13435−13446.
(29) Shen, M. R.; Downing, K. H.; Balhorn, R.; Hud, N. H. Nucleation of DNA condensation by static loops: formation of DNA toroids with reduced dimensions. *J. Am. Chem. Soc.* **2000**, *122*, 4833−4834.
(30) Hashem, A.; Hossain, M. A. M.; Marlinda, A. R.; Al Mamun, M.; Simarani, K.; Johan, M. R. Nanomaterials based electrochemical nucleic acid biosensors for environmental monitoring: A review. *Appl. Surf. Sci. Adv.* **2021**, *4*, No. 100064.

https://doi.org/10.1021/acsomega.1c06926
ACS Omega 2022, 7, 15404−15410